Available online at www.sciencedirect.com
SCIENCE DIRECT®
Journal of Magnetic Resonance 169 (2004) 270–278
JMR Journal of Magnetic Resonance
www.elsevier.com/locate/jmr

Spin-lattice relaxation and a fast T_1-map acquisition method in MRI with transient-state magnetization

Jung-Jiin Hsu*,[1] and Irving J. Lowe

Department of Physics and Astronomy, University of Pittsburgh, Pittsburgh, PA 15260, USA
Pittsburgh NMR Center for Biomedical Research, Carnegie Mellon University and University of Pittsburgh, 4400 Fifth Avenue, Pittsburgh, PA 15213, USA

Received 1 January 2004; revised 9 April 2004
Available online 7 June 2004

Abstract

The magnetization under the spin-lattice relaxation and the nuclear magnetic resonance radiofrequency (RF) pulses is calculated for a signal RF pulse train and for a sequence of multiple RF pulse-trains. It is assumed that the transverse magnetization is zero when each RF pulse is applied. The result expressions can be grouped into two terms: a decay term, which is proportional to the initial magnetization M_0, and a recovery term, which has no M_0 dependence but strongly depends on the spin-lattice relaxation and the equilibrium magnetization M_{eq}. In magnetic resonance pulse sequences using magnetization in transient state, the recovery term produces artifacts and can seriously degrade the function of the preparation sequence for slice selection, contrast weighting, phase encoding, etc. This work shows that the detrimental effect can be removed by signal averaging in an eliminative fashion. A novel fast data acquisition method for constructing the spin-lattice relaxation (T_1) map is introduced. The method has two features: (i) By using eliminative averaging, the curve to fit the T_1 value is a decay exponential function rather than a recovery one as in conventional techniques; therefore, the measurement of M_{eq} is not required and the result is less susceptible to the accuracy of the inversion RF pulse. (ii) The decay exponential curve is sampled by using a sequence of multiple pulse-trains. An image is reconstructed from each train and represents a sample point of the curve. Hence a single imaging sequence can yield multiple sample points needed for fitting the T_1 value in contrast to conventional techniques that require repeating the imaging sequence for various delay values but obtain only one sample point from each repetition.

Keywords: Spin-lattice relaxation; T_1 map; Fast imaging; Transient-state magnetization; RUFIS

1. Introduction

The basic building block of a nuclear magnetic resonance (NMR) pulse sequence consists of a radiofrequency (RF) pulse, acquisition of NMR induction signal, and a delay for magnetization recovery. Many NMR and NMR imaging (MRI) techniques complete the data collection by repeated use of the building block, i.e., by using a pulse train. In such techniques, the experiment time can be shortened by reducing the RF pulse length and the delay for recovery. If the reduced recovery delay is shorter than the time needed to fully recover the magnetization, the magnetization will not reach the equilibrium state during the execution of the pulse train.

Each RF pulse transforms partial longitudinal magnetization into the transverse plane. The successive application of RF pulses gradually consumes the longitudinal magnetization while, conversely, the spin-lattice relaxation recovers the magnetization towards the equilibrium state. During the pulse train, the longitudinal magnetization evolves from the initial state through the transient state and then to the steady state [1] in which the competing consumption and recovery reach a

* Corresponding author. Present address: Lucas MRS/I Center, Stanford University School of Medicine, 1201 Welch Road MC 5488, Stanford, CA 94305-5488, USA. Fax: 1-650-723-5795.
E-mail address: jjhsu@stanford.edu (J.-J. Hsu).
[1] Also known as Jason Hsu.

1090-7807/$ - see front matter © 2004 Elsevier Inc. All rights reserved.
doi:10.1016/j.jmr.2004.05.001

balance and the magnetization is a constant when each RF pulse is applied. But in the transient state, the magnetization fluctuates; consequently, the NMR signals, which are proportional to the volume integral of the magnetization, are unevenly weighted; this is the main reason that most of the NMR and MRI methods start the signal acquisition after a steady state is established.

But problems with the steady-state methods exist: (i) a large number of pulses are required to establish a steady state. For example, with a 5° flip-angle pulse, a 5-ms recovery delay, and a sample of spin-lattice relaxation time $T_1 = 500\,\text{ms}$, more than 300 RF pulses are required for the magnetization to reach 95% of the steady-state value [2]. Not only is it a waste of time in fast imaging [3–5], but also the excessive RF power deposition to the imaged subject can be a serious concern. (ii) Further, a preparation sequence is usually added ahead of the pulse train to make the magnetization sensitive to relaxations, diffusion, etc., or to perform slice selection or phase encoding to the magnetization. For example, a preparation sequence for spatial encoding makes the magnetization a function of spatial coordinates so that the NMR signals from the pulse train will contain the coordinate information. But, as it will be shown in Section 4.1, the preparation sequence is useless if the magnetization reaches the steady state because in the steady state the magnetization is no longer a function of the parameters that the preparation sequence is designed for. (iii) There are situations where the pulse train must be segmented to insert, e.g., lipid NMR signal suppression [6], which adds to the difficulties of maintaining a steady state. (iv) Many dynamical systems simply do not have steady-state magnetization. For example, a selected slice of flow does not stay for steady state.

Methods utilizing transient-state magnetization do not have the above drawbacks but the fluctuating magnetization results in unevenly weighted signals and the spin-lattice relaxation degrades the effect of the preparation sequence [2,7–10]. To obtain accurate results from transient-state methods, the present work is interested in solving these problems. Because the application of an RF pulse couples the longitudinal and the transverse magnetization, a full theoretical analysis will be very involved except for pulse trains in which the phase of the magnetization is balanced [11]. Hence, the present work will focus on the condition that the transverse magnetization is zero at the time each RF pulse is applied. The condition is satisfied if the transverse-relaxation time is much shorter than the repetition delay or the flip angle of the RF pulses is low. First, a mathematical expression describing the NMR signals of a pulse train in the transient state is derived (Section 3). The mathematical expression for the NMR signals can be grouped into two terms; one depends on the initial magnetization, which contains the information encoded by the preparation sequence, and the other does not depend on the initial magnetization but is the origin of the problems. Therefore by using signal averaging with different initial magnetization the problems can be eliminated as shown in Section 4. In addition, based on the theoretical analysis, a novel time-saving data acquisition method [12,13] for constructing a spin-lattice relaxation map (T_1 map) is also introduced in this work (Section 4). The MRI pulse sequence used in this work for experimental examination and demonstration is described in Section 2 and detailed in Appendix A.

2. Method

The transient-state MRI method used experimentally in the present study is the rotating ultra-fast imaging sequence (RUFIS) [14,15], which is depicted in Fig. 1. The preparation sequence performs slice selection and transverse-relaxation weighting. RUFIS contains a train of low flip-angle RF pulses. The direction of the read gradient, θ, is set at a different value for each RF pulse so the free induction decays (FIDs) are radial samples in the image conjugate domain (the k-space). The image is reconstructed from the radial samples by filtered back-projection. At the end of RUFIS, an RF pulse is applied to acquire an auxiliary signal with zero read gradient. The details of RUFIS and the image reconstruction are given in Appendix A.

Unless otherwise noted, RUFIS in this work contained 64 RF pulses and scanned the k-space for $\theta \in [0, 2\pi)$. The read gradient was set to its first value 3 ms prior to the commencement of the pulse train to dephase the remaining transverse magnetization. The central 1-cm slice of the imaged subject was selected using a five-lobe sinc shape (i.e., truncated at $\pm 3\pi$) RF pulse (1.55 ms long). The flip angle α was $6°_{+x}$ or 8 μs long. Each FID was sampled at one complex point per μs for 128 points. For the back-projection reconstruction, the k-space data set was equivalent to the discrete Fourier transformation matrix size of 256×256. The

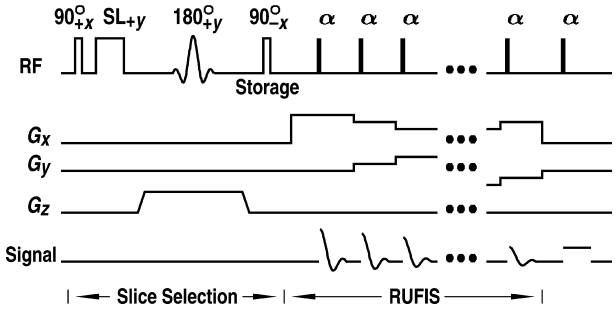

Fig. 1. Slice selective RUFIS. SL is a spin-lock pulse and α's are low flip-angle pulses.

NMR probe [15] and the gradient coils were in-house-made. The RF pulses, pre-emphasized gradient outputs, and the Zeeman-field (B_0) compensation were generated by a digital console. All of the experiments were performed at 2.35 T.

3. Theory

In this section, the longitudinal magnetization with an arbitrary initial value and under the spin-lattice relaxation is calculated for a single pulse train and for a sequence of multiple pulse-trains; the latter is for an interesting application of relaxation-time mapping to be introduced in Section 4.3, which utilizes the pulse trains to produce a time series of images.

In this work, M_{eq} denotes the thermal equilibrium magnetization, and M_0 the initial magnetization at the beginning of the first RF pulse.

3.1. Single RF pulse train

Consider a train of uniformly spaced RF pulses. Let $M_{z(n)}(\tau)$, $n > 0$, represent the longitudinal magnetization at time τ following the nth RF pulse. The recovery of the longitudinal magnetization by the spin-lattice relaxation is described by

$$M_{z(n)}(\tau) = M_{z(n)}(0)\mathrm{e}^{-\tau/T_1} + M_{\text{eq}}(1 - \mathrm{e}^{-\tau/T_1}). \tag{1}$$

This equation is the solution to the Bloch equations in the absence of the RF field. If the transverse magnetization is zero (i.e., irreversibly relaxed) and if the pulse length is negligible, the effect of an RF pulse of flip angle α is to produce a transverse component

$$M_{\perp(n)}(0) = M_{z(n-1)}(\Delta)\sin\alpha, \tag{2}$$

and to change the longitudinal component to be

$$M_{z(n)}(0) = M_{z(n-1)}(\Delta)\cos\alpha, \tag{3}$$

where Δ is the time between the RF pulses.

The weight of the nth NMR signal in the pulse train is determined by $M_{\perp(n)}(0)$. Given the initial longitudinal magnetization M_0, one can obtain the expression for $M_{\perp(n)}(0)$ by iteratively substituting Eqs. (1)–(3). For the first RF pulse, $M_{\perp(1)}(0) = M_0\sin\alpha$ by using Eq. (2) with $M_{z(0)}(\Delta) = M_0$. To calculate for the second RF pulse, $M_{z(1)}(\Delta)$ is needed, which can be obtained by substituting Eq. (3) into Eq. (1); then from Eq. (2) with $n = 2$,

$$M_{\perp(2)}(0) = [M_0E_{1\Delta}\cos\alpha + M_{\text{eq}}(1 - E_{1\Delta})]\sin\alpha, \tag{4}$$

where $E_{1\Delta} = \mathrm{e}^{-\Delta/T_1}$. Each iteration for the next RF pulse multiplies a factor $(E_{1\Delta}\cos\alpha)$ and adds a term $M_{\text{eq}}(1 - E_{1\Delta})$ to the expression in the square brackets of Eq. (4). Finally, the desired expression for $M_{\perp(n)}(0)$ is obtained

$$\begin{aligned} M_{\perp(n)}(0) = \Big\{ & M_0(E_{1\Delta}\cos\alpha)^{n-1} + M_{\text{eq}}(1 - E_{1\Delta}) \\ & \times[(E_{1\Delta}\cos\alpha)^{n-2} + (E_{1\Delta}\cos\alpha)^{n-3} \\ & + \cdots + 1]\Big\}\sin\alpha, \end{aligned} \tag{5}$$

or, with the formula of the geometric series sum,

$$\begin{aligned} M_{\perp(n)}(0) = \Bigg[& M_0(E_{1\Delta}\cos\alpha)^{n-1} \\ & + M_{\text{eq}}(1 - E_{1\Delta})\frac{1 - (E_{1\Delta}\cos\alpha)^{n-1}}{1 - E_{1\Delta}\cos\alpha}\Bigg]\sin\alpha. \end{aligned} \tag{6}$$

A similar approach by iterative substitution can be found in [2]. Keep in mind that M_z, $M_\perp$, M_{eq}, M_0, and T_1 are functions of spatial coordinates if the subject is heterogeneous.

3.2. Multiple RF pulse-trains

Consider a sequence of multiple trains; each train has N RF pulses as shown in Fig. 2. The first pulse train starts after a delay D_1 from the time point at which M_0 is specified, and the ith pulse train, $i > 1$, starts after a delay D_i from the end of the last train. The end of a train is defined as time Δ past the last pulse of the train. In what follows, $E_{1D_i} \equiv \mathrm{e}^{-D_i/T_1}$, and (i, n) in the subscript labels the quantities for the nth RF pulse of the ith pulse train.

For the first pulse train, Eq. (6) should be rewritten to include the spin-lattice relaxation during D_1. Therefore M_0 in Eq. (6) is substituted by $M_0E_{1D_1} + M_{\text{eq}}(1 - E_{1D_1})$ as described by Eq. (1), that is

$$M_{\perp(1,n)}(0) = \left[M_0(E_{1\Delta}\cos\alpha)^{n-1}E_{1D_1} + C_1(n)\right]\sin\alpha, \tag{7}$$

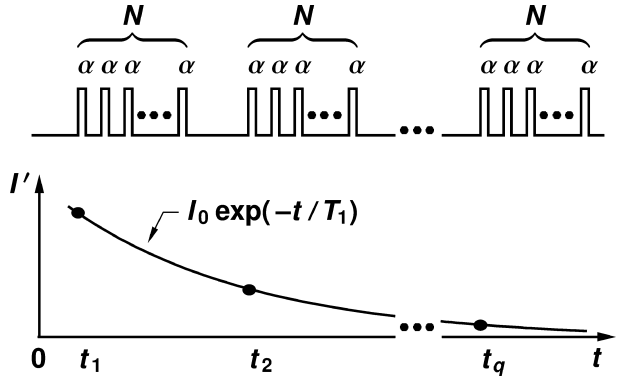

Fig. 2. Schematic representation of sampling a decay exponential curve of time constant T_1 by a sequence of q RF pulse-trains (with eliminative averaging). An image is reconstructed from each train and represents a sample point on the curve.

where

$$C_1(n) = M_{\mathrm{eq}}(1 - E_{1D_1})(E_{1\Delta}\cos\alpha)^{n-1} + M_{\mathrm{eq}}(1 - E_{1\Delta}) \times \frac{1 - (E_{1\Delta}\cos\alpha)^{n-1}}{1 - E_{1\Delta}\cos\alpha}. \quad (8)$$

At the end of the first pulse train, the longitudinal magnetization is given by [cf. Eq. (1)]

$$M_{z(1,N)}(\Delta) = M_{z(1,N)}(0)E_{1\Delta} + M_{\mathrm{eq}}(1 - E_{1\Delta}) \quad (9)$$

with $M_{z(1,N)}(0)$ given by [cf. Eq. (7)]

$$M_{z(1,N)}(0) = \left[M_0(E_{1\Delta}\cos\alpha)^{N-1}E_{1D_1} + C_1(N)\right]\cos\alpha. \quad (10)$$

For the second pulse train, $M_{\perp(2,n)}(0)$ can be calculated by reusing Eqs. (7) and (8) with $M_{\perp(1,n)}(0)$ replaced by $M_{\perp(2,n)}(0)$, E_{1D_1} replaced by E_{1D_2}, and M_0 substituted by $M_{z(1,N)}(\Delta)$ of Eq. (9). By iterating the calculation, a general formula for the nth RF pulse of the ith train, $i > 1$, is arrived:

$$M_{\perp(i,n)}(0) = \left[M_0(E_{1\Delta}\cos\alpha)^{(i-1)N+n-1}E_{1D_1}E_{1D_2}\cdots E_{1D_i} + C_i(n)\right]\sin\alpha \quad (11)$$

or

$$M_{\perp(i,n)}(0) = \left[M_0(E_{1\Delta}\cos\alpha)^{n-1}\cos^{(i-1)N}\alpha\, e^{-t_i/T_1} + C_i(n)\right]\sin\alpha, \quad (12)$$

with

$$C_i(n) = C_{i-1}(N)E_{1D_i}(E_{1\Delta}\cos\alpha)^n + M_{\mathrm{eq}}(1 - E_{1\Delta}E_{1D_i}) \times (E_{1\Delta}\cos\alpha)^{n-1} + M_{\mathrm{eq}}(1 - E_{1\Delta})\frac{1 - (E_{1\Delta}\cos\alpha)^{n-1}}{1 - E_{1\Delta}\cos\alpha}, \quad (13)$$

where t_i is the time when the ith pulse train is started relative to the time point at which M_0 is specified. If $i = 1$, Eqs. (7) and (8) are used. The expressions for $C_i(n)$'s are complicated, but one only needs to remember that they are not functions of M_0. For convenience, the first term in the square brackets of Eqs. (6), (7), and (12) is referred to as the M_0 *term* and the second term as the *recovery term*.

4. Results and discussion

4.1. Steady-state magnetization revisited

Eq. (6) describes the transverse component of the magnetization as a function of the number of RF pulses n. The non-trivial steady state (SS) is achieved when n is infinitely large and then Eq. (6) becomes

$$M_{\perp}^{\mathrm{SS}}(0) = M_{\mathrm{eq}}\frac{1 - E_{1\Delta}}{1 - E_{1\Delta}\cos\alpha}\sin\alpha, \quad (14)$$

which agrees with the formula of Ernst et al. [1,16], who started from the recursion relation of the steady state (also see [17]). Note that the M_0 dependence is gone. Consequently, if a preparation sequence is performed prior to the pulse train to encode information to the initial magnetization M_0, the signals acquired in the steady state do not carry the encoded information.

4.2. Transient-state imaging

Accurately recalling the information encoded to M_0 from the transient-state signals is feasible only if the recovery term in Eq. (6) is negligible in comparison with the M_0 term, which is not the case when n is large or T_1 is short. Removal of the recovery term by post-processing is possible if M_{eq} and T_1 are known a priori. But the determination of M_{eq} and T_1, both being functions of spatial coordinates, requires extra works and adds to the difficulties. In this section, an experimental technique that can separate the M_0 and the recovery terms without post-processing is described, and the artitact due to the recovery term is demonstrated.

Consider two experiments: one is performed regularly, but the other is performed with the sign of M_0 inverted. For pulse sequences similar to that shown in Fig. 1, the sign inversion can be accomplished by executing the storage RF pulse with the phase $+x$. Subtraction between the two data sets gives [cf. Eq. (6)]

$$\tilde{M}_{\perp(n)}(0) \equiv M_{\perp(n)}(0)\big|_{M_0} - M_{\perp(n)}(0)\big|_{-M_0} = 2M_0(E_{1\Delta}\cos\alpha)^{n-1}\sin\alpha. \quad (15)$$

The recovery term is eliminated. Similarly, if the two data sets are added, only the recovery term remains. Then the two terms are separated.

To compare the recovery term and the M_0 term in their magnitude as the number of pulses increases, a series of RUFIS experiments were performed; each experiment had a different number of RF pulses and a regular or an inverted M_0. The sample (detailed in Section 4.3) was composed of liquids of various T_1 values in the range from 0.2 to 1.1 s. The direction of the RUFIS read gradient was held constant. By using the auxiliary signal at the end of RUFIS (see Fig. 1 and Section 2), the recovery-to-M_0-term ratio was calculated. For $n = 0$, 16, 32, 48, and 64, the ratios were 0.05, 0.10, 0.15, 0.19, and 0.24, respectively. The ratio will vary from study to study, e.g., the thinner the slice width and/or the shorter the T_1, the greater the ratio; nevertheless, the present example has shown that the recovery effect may not be negligible in transient-state methods.

According to Eq. (15), if an image is to be reconstructed from the NMR signals of the pulse train, each signal needs to be multiplied by the normalization factor $(E_{1\Delta}\cos\alpha)^{1-n}$ to even the signals. This factor is T_1-dependent; therefore, the normalization could be

impractical for heterogeneous subject because the NMR signal is in fact determined by the volume integral of the transverse magnetization. Nevertheless, if $\Delta \ll T_1$ (e.g., $\Delta = 180\,\mu s$ in this work and $T_1 \sim 800\,ms$ is common in vivo), then $E_{1\Delta}$ can be replaced by one or by a representative constant of the imaged subject.

MRI with improved signal-to-noise ratio is usually achieved by averaging repeated experiments. As suggested by the above analysis, employing inverted M_0 for half of the total number of repetitions can eliminate the spin-lattice relaxation effect and will be referred to as *eliminative averaging* in the following discussion in contrast to the regular *accumulative averaging* which has no M_0 inversion. Fig. 3 shows two RUFIS images of a kiwi fruit with T_1 determined in a separate experiment to be in the range from 0.9 to 1.4 s. The read gradient was $G_{read} = 5.51\,G/cm$. A delay was inserted in the preparation sequence such that the spin-lock and the storage RF pulses were separated by 102 ms to let M_0 be modulated by the transverse relaxation. Hence the images were meant to be transverse-relaxation (T_2^*) weighted. For each image, the range of the intensity was linearly scaled to cover the full gray scale. As can be seen in the figure, without eliminating the spin-lattice relaxation effect, the accumulative-averaging image can hardly show proper contrast. The present MRI system has an RF leak [10]. The Fourier spectra of the signals from an empty probe have a sharp peak at 57 kHz off the NMR frequency. The leak signal is responsible for the swirly scars at the outline of the fruit in the accumulative-averaging image. It is interesting to note that, since eliminative averaging is equivalent to a phase cycling technique, the eliminative averaging can effectively remove the leak signal.

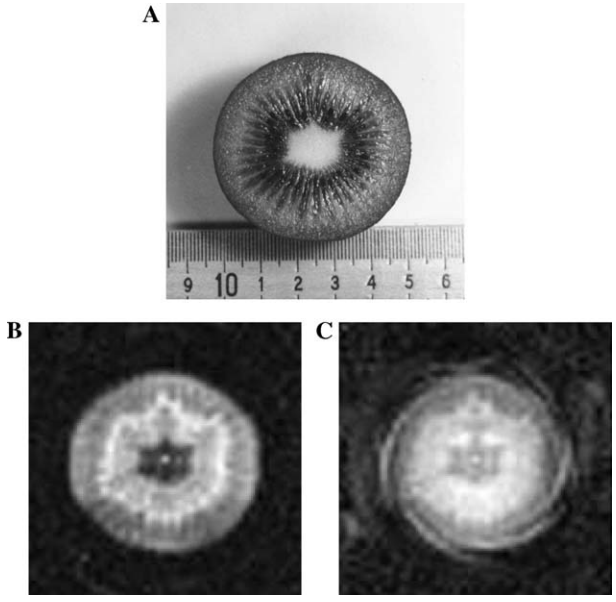

Fig. 3. Photograph (A) and RUFIS MRI images (B and C; matrix size: 45×45) of a kiwi fruit. For (B), eliminative averaging was used to remove the spin-lattice relaxation effect while (C) was obtained by regular (accumulative) averaging.

The magnitude of the spin-lattice relaxation effect was not expected for the pulse train method FLASH [18] in which a steady-state expression was used to analyze the transient-state method. However, Coremans et al. [8] found that the spin-lattice relaxation causes serious error in quantitative FLASH imaging but can be eliminated by a subtraction sequence, i.e., eliminative averaging.

Fig. 4 further shows a series of T_2^* weighted images using RUFIS with eliminative averaging. Each image was acquired with a different delay in the preparation sequence. These images suggest that RUFIS with eliminative averaging is capable of delivering the effect of the preparation sequence.

4.3. Time-saving T_1-map imaging

Eq. (12) describes the transient-state magnetization of a sequence of multiple pulse-trains. If two experiments are performed for eliminative averaging, the resulting NMR signal for the nth RF pulse in the ith pulse train is proportional to the volume integral of

$$\tilde{M}_{\perp(i,n)}(0) = 2M_0(E_{1\Delta}\cos\alpha)^{n-1}\cos^{(i-1)N}\alpha\, e^{-t_i/T_1}\sin\alpha. \tag{16}$$

Recall that t_i is the time when the ith pulse train is started relative to the time at which M_0 is specified, and N is the number of RF pulses in a train. If the signals in a pulse train, after normalization, are used to reconstruct one image I_i, then Eq. (16) implies

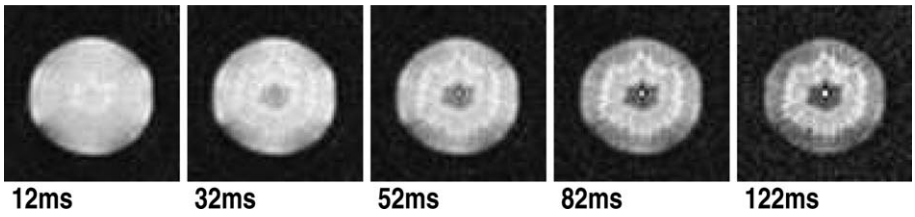

Fig. 4. Transverse-relaxation weighted images of a kiwi fruit using RUFIS with eliminative averaging. The labels indicate the time span of the preparation sequence. The image size is 45×45.

$$I_i = I_0 \cos^{(i-1)N} \alpha \, e^{-t_i/T_1} \quad (17)$$

or

$$I'_i = I_0 \, e^{-t_i/T_1}, \quad (18)$$

where $I'_i = I_i \cos^{(1-i)N} \alpha$. Eq. (18) is an exponential decay with a time constant of the sample's T_1; it suggests a time-saving method for acquiring data to produce a T_1 map as illustrated in Fig. 2, in which an imaging sequence of multiple pulse-trains is performed and repeated for eliminative averaging. The image reconstructed from the ith pulse train represents the sample point on the decay curve at time t_i. Then a T_1 map can be obtained by fitting these images to decay exponential functions. If the pulse train is much shorter than T_1, the imaging sequence can accommodate as many pulse trains as the signal-to-noise ratio allows, and one can obtain multiple sample points of the decay curve in one batch. Conventional methods such as the inversion-recovery would obtain only one sample point at a time.

Fig. 5 shows T_1 maps obtained from the suggested method. Following the slice selection, the imaging sequence consisted of six RUFIS trains with a constant inter-train delay of 180 ms. Each RUFIS train took 12 ms. The imaged subject (also used in Section 4.2) was constructed with seven glass vials; each of them is of 4.5-cm height and 1.2-cm diameter and was filled with liquid of T_1 value shown in Table 1. Fig. 5 shows a T_1 map from 16 repetitions with a delay of 8 s before each repetition to allow recovery of the magnetization. In the T_1 map, the variation of the intensity among the vials does follow the reference values shown in Table 1. Each reference value was obtained by individually measuring a 0.2-cm^3 sample using the inversion-recovery, or 180°–τ–90°, pulse sequence with a solenoid coil and the same MRI system. For each liquid, 10 sample points were obtained for curve fitting; experimentally, each point took four repetitions with 8-s repetition delays.

To compare the T_1 map with the reference values, the T_1 values of the pixels belonging to the same vial are averaged, and the average is tabulated in Table 1 together with the standard deviation in the parentheses. As shown in column A, the MRI results are in very good agreement with the reference values. Even with only two scans, the present method can produce reasonably accurate results as shown in Fig. 5 and in column B of Table 1. The two-scan experiment took only 4.2 s, including a 2-s recovery delay. According to Eq. (18), the ith image needs to be multiplied by the factor $\cos^{(1-i)N} \alpha$ before the exponential-curve fitting. Therefore, the error in the images obtained from later pulse-trains can be amplified by the multiplication; the accuracy of the flip angle α can also affect the measurement if the flip angle is large. The two-scan experiment has lower signal-to-noise ratio and, therefore, has larger standard deviations as expected.

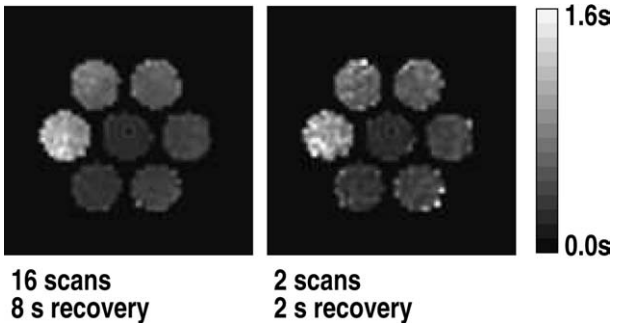

Fig. 5. Spin-lattice relaxation (T_1) maps by multiple pulse-train MRI. The sample liquid at the center is numbered 7; the others, from the 9-o'clock position and clockwise, are numbered 1–6.

Table 1
Spin-lattice relaxation times (s) measured by multiple pulse-train MRI and the reference values by the conventional spectroscopy technique

Sample	Reference value	MRI	
		A	B
1	1.02	1.07 (0.20)	1.01 (0.25)
2	0.62	0.66 (0.11)	0.64 (0.15)
3	0.46	0.53 (0.05)	0.56 (0.11)
4	0.37	0.37 (0.04)	0.37 (0.07)
5	0.31	0.33 (0.03)	0.35 (0.06)
6	0.27	0.27 (0.02)	0.28 (0.06)
7	0.21	0.22 (0.03)	0.22 (0.04)

The numbers in the parentheses are the standard deviations. Columns A and B are obtained from the 16-scan and the 2-scan experiment, respectively.

Other multiple-point T_1-map techniques [19–23] and the inversion-recovery method require one or more of the following conditions: $M_0 = 0$, $-M_{eq}$, or $-M_z^{SS}$, or the determination of M_{eq} or M_z^{SS}. The present method does not have these requirements.

4.4. Remarks

In this work, the two sets of experiments for eliminative averaging are performed with initial magnetization M_0 and $-M_0$, respectively; the latter is achieved by an inversive RF pulse. However, if the second set starts with $-\beta M_0$, where β is an arbitrary constant, the coefficient $2M_0$ in Eqs. (15) and (16) becomes $(1+\beta)M_0$ and the eliminative averaging still produces a decay exponential function with the time constant unchanged. Thus, if the measurement concerns only the T_1 value, the second experiment does not require the magnetization exactly equal $-M_0$. Therefore, an inversive RF pulse not perfectly at the theoretical flip-angle is tolerable as long as the transverse magnetization is zero prior to the pulse train. Similarly, full recovery of the magnetization before the second experiment, although resulting in higher signal-to-noise ratio, is not necessary.

To sample the exponential curve of Eq. (18), the present work uses a sequence of multiple pulse-trains. As it can be seen in Fig. 2 with $N = 1$, the concept can be extended to MRI methods which acquire one image with a single RF pulse (e.g., echo planar imaging, spiral scan, etc.). One can verify this with Eqs. (16) and (17) by setting $N = 1$ and $n = 1$, and finds that Eq. (18) is still preserved.

5. Conclusion

Theoretically, the longitudinal magnetization with arbitrary initial value M_0 and under the spin-lattice relaxation is calculated for a signal RF pulse train and for a sequence of multiple RF pulse-trains. It is assumed that the transverse magnetization is zero when each RF pulse is applied. The general expressions of the magnetization can be grouped into two terms: a decay term, which is proportional to M_0, and a recovery term, which has no M_0 dependence but is strongly affected by the spin-lattice relaxation.

Experimentally, the results from the rotating ultra-fast imaging sequence (RUFIS) suggest that in methods using transient-state magnetization the contribution of spin-lattice relaxation to the NMR signals is not negligible. The relaxation can seriously degrade the function of the preparation sequence for slice selection, contrast weighting, phase encoding, etc. Nevertheless, the spin-lattice relaxation effect can be removed by eliminative averaging in which half of the total number of repetitions are performed with an inverted M_0 and the data are subtracted from that of the other half repetitions.

The present work introduces a time-saving data acquisition method for constructing the T_1 map. The method has two features: (i) By using eliminative averaging, the curve to fit for the T_1 value is a decay exponential function Eq. (18). Conventional transient-state techniques, such as inversion-recovery, will involve fitting a recovery exponential function, e.g., Eq. (1), which requires the determination of the equilibrium magnetization M_{eq} and/or $M_0 = 0$, or $-M_{\text{eq}}$. The present method is not subject to these requirements and the result is less susceptible to the accuracy of the flip angle of the inversion RF pulse. (ii) The decay exponential is sampled by using a sequence of multiple pulse-trains. An image is reconstructed from each pulse train and represents the sample point at the time when that pulse train is started (see Fig. 2). Hence a single imaging sequence can yield multiple sample points needed for data fitting to obtain the T_1 map. Conventional techniques require repeating the imaging sequence for various values of the recovery delay but each repetition obtains only one sample point. The multiple pulse-train method is tested by using RUFIS and is found to be effective to produce accurate T_1 maps.

Acknowledgments

The experiments were performed at the Pittsburgh NMR Center for Biomedical Research. The Center is supported by NIH Grant P41RR-03631 from the National Center for Research Resources as an NIH-supported resource center. The remark on non-perfect inversion of the initial magnetization is due to an enjoyable discussion with Professor Gary H. Glover of Stanford University.

Appendix A

This appendix describes in detail the NMR imaging pulse sequence shown in Fig. 1. The first $90°_{+x}$ pulse turns the magnetization into the transverse plane; if the flip angle is not at perfect 90°, the spin-lock pulse, implemented as a long (3 ms) rectangular RF pulse, "dephases" the zx-plane component of the magnetization. The slice gradient G_z and the shaped $180°_{+y}$ RF pulse dephase the transverse magnetization and refocus only that inside the desired slice. The succeeding $90°_{-x}$ *storage pulse* turns the transverse magnetization back along the longitudinal axis. Depending on the purpose of the study, the preparation sequence may include additional segments for spatial or velocity encoding; the encoded information will be stored as the longitudinal magnetization by the storage pulse. The main part in Fig. 1 is the rotating ultra-fast imaging sequence (RUFIS) [14,15]. RUFIS contains a train of low flip-angle RF pulses (flip angle α) with the read gradient given by $G_x = G_{\text{read}} \cos\theta$ and $G_y = G_{\text{read}} \sin\theta$; the FID signal is recorded immediately after each RF pulse. The polar direction of the read gradient, θ, is kept constant during the RF transmission and signal reception period and is set to a new value before the application of the next RF pulse. The angle θ varies through equal-spaced values in $[0, 2\pi)$ so the image conjugate domain (the k-space) is sampled radially by the FIDs. The FIDs need to be normalized by the factor $(E_{1\Delta} \cos\alpha)^{1-n}$ as discussed after Eq. (15). In a RUFIS train, the gradient outputs G_x and G_y step gradually; therefore the induced eddy current is expected to be small. Other features of RUFIS include that acquisition of the FID eliminates the time needed to refocus an echo, and the information encoded in the preparation sequence is preserved in the longitudinal rather than the transverse magnetization until recalled by each RF pulse. Both reduce the time the magnetization stays in the transverse plane, making RUFIS a method less susceptible to de-coherence due to field inhomogeneity and time varying factors such as diffusion, motion, flow, etc.

At the end of RUFIS, the read gradient is set to zero; then an additional α RF pulse is executed to produce an auxiliary NMR signal (Fig. 1) for the purpose of the

signal extrapolation of the initial portion of each RUFIS FID. The initial portion cannot be recorded because the receiver is blanked for the RF transmission. When being tilted by the RF pulse under a non-zero read gradient, the magnetization is also precessing relative to the rotating frame, generating imaging signal; but the signal cannot be recorded by the blanked receiver. The initial portions must be recovered before the FIDs can be used in the image reconstruction. Recently, a simple extrapolation formula has been given by Hsu and Lowe [15] to treat the problem of incomplete signal acquisition. It was found that if the data point at the origin of the FID is known and is entered to the extrapolation computation, the extrapolated signal is almost identical to the actual FID. The auxiliary signal is to represent the data at the FID origin since the signal is acquired at zero gradient and all decay mechanisms of the NMR signal such as transverse relaxation and field inhomogeneity are negligible during the very short period of the receiver blanking and signal acquisition (e.g., $\sim$150 μs). In this work, the auxiliary signal was normalized the same way as the RUFIS FIDs; then the average value S_{aux} of the data points of the normalized auxiliary signal was calculated. However, S_{aux} cannot be used directly for the origin of the normalized RUFIS FIDs because, while the auxiliary RF pulse flips the magnetization uniformly across the imaged subject, the flip angle by the RF pulses of RUFIS is not uniform due to the non-zero read gradient. For a low flip-angle RF pulse, the spatial profile of the flip angle can be approximated by a sinc function, $\text{sinc}(x) \equiv \sin(x)/x$, along the read gradient direction. For a slice with a circular plane and centered at the gradient center, the value S_0 for the origin of the FID with non-zero gradient is

$$S_0 = S_{\text{aux}} \frac{\int_0^R \text{sinc}\left(\frac{L}{2}r\right)\sqrt{R^2 - r^2}\,\mathrm{d}r}{\int_0^R \sqrt{R^2 - r^2}\,\mathrm{d}r}, \tag{A.1}$$

where L is the RF pulse length divided by the receiver sampling period and R is the radius of the imaged subject divided by the width corresponding to the Nyquist frequency and multiplied by π. The integral in the denominator is simply the area of a circle and that in the numerator is the area weighted by a sinc function along the diameter. More symmetric and homogeneous is the imaged subject, more accurately S_0 approximates the origin of the RUFIS FIDs.

In Hsu and Lowe [15], a pulse sequence was designed to acquire a stimulated spin echo (SSE) to examine the FID. In this work, the SSE pulse sequence determined the number of blanked data points in the FID, which is needed in the extrapolation computation. This number is considered a constant when the identical pulse sequence and parameters are used on the same MRI system. Therefore, once the number of blanked data is determined, the SSE pulse sequence is not repeated for routine RUFIS experiments. The signal recovery and the image reconstruction from RUFIS FIDs are detailed in Hsu and Lowe [15].

References

[1] R.R. Ernst, W.A. Andrew, Application of Fourier transform spectroscopy to magnetic resonance, Rev. Sci. Instrum. 37 (1966) 93–102.

[2] W. Hänicke, K.D. Merboldt, D. Chien, M.L. Gyngell, H. Bruhn, J. Frahm, Signal strength in subsecond FLASH magnetic resonance imaging: the dynamic approach to steady state, Med. Phys. 17 (1990) 1004–1010.

[3] B.A. Hargreaves, S.S. Vasanawala, J.M. Pauly, D.G. Nishimura, Characterization and reduction of the transient response in steady-state MR imaging, Magn. Reson. Med. 46 (2001) 149–158.

[4] R.F. Busse, S.J. Riederer, Steady-state preparation for spoiled gradient echo imaging, Magn. Reson. Med. 45 (2001) 653–661.

[5] V.S. Deshpande, S.M. Shea, G. Laub, O.P. Simonetti, J.P. Finn, D. Li, 3D magnetization-prepared true-FISP: a new technique for imaging coronary arteries, Magn. Reson. Med. 46 (2001) 494–502.

[6] K. Scheffler, O. Heid, J. Henning, Magnetization preparation during the steady state: fat-saturated 3D TrueFISP, Magn. Reson. Med. 45 (2001) 1075–1080.

[7] A.E. Holsinger, S.J. Riederer, The importance of phase-encoding order in ultra-short TR snapshot MR imaging, Magn. Reson. Med. 16 (1990) 481–488.

[8] J. Coremans, M. Spanoghe, L. Budinsky, J. Sterckx, R. Luypaert, H. Eisendrath, M. Osteaux, A comparison between different imaging strategies for diffusion measurements with the centric phase-encoded turboFLASH sequence, J. Magn. Reson. 124 (1997) 323–342.

[9] C.F.M. Williams, T.W. Redpath, Sources of artifact and systematic error in quantitative snapshot FLASH imaging and methods for their elimination, Magn. Reson. Med. 41 (1999) 63–71.

[10] J.-J. Hsu, I.J. Lowe, Spatial three dimensional imaging using RUFIS, in: Proceedings of the International Society for Magnetic Resonance in Medicine, vol. 8, International Society for Magnetic Resonance in Medicine, 2000, p. 680.

[11] K. Scheffler, On the transient phase of balanced SSFP sequences, Magn. Reson. Med. 49 (2003) 781–783.

[12] J.-J. Hsu, I.J. Lowe, Time-saving T_1-map imaging, in: The 43rd Experimental Nuclear Magnetic Resonance Conference, April 14–19, 2002, Asilomar Conference Center, Pacific Grove, CA, USA, 2002.

[13] J.-J. Hsu, Fast nuclear magnetic resonance imaging with transient-state magnetization and a cylindrical sampling scheme, Ph.D. dissertation, University of Pittsburgh, Pittsburgh, PA, April 2002.

[14] D.P. Madio, I.J. Lowe, Ultra-fast imaging using low flip angles and FIDs, Magn. Reson. Med. 34 (1995) 525–529.

[15] J.-J. Hsu, I.J. Lowe, Signal recovery in free induction decay imaging using a stimulated spin echo, Magn. Reson. Med. 47 (2002) 409–414.

[16] R.R. Ernst, G. Bodenhausen, A. Wokaun, Principles of Nuclear Magnetic Resonance in One and Two Dimensions, Clarendon Press, Oxford, UK, 1987.

[17] G. Brix, L.R. Schad, M. Deimling, W.J. Lorenz, Fast and precise T_1 imaging using a TOMROP sequence, Magn. Reson. Imaging 8 (1990) 351–356.

[18] A. Haase, Snapshot FLASH MRI. Application to T1, T2, and chemical-shift imaging, Magn. Reson. Med. 13 (1990) 77–89.

[19] D.C. Look, D.R. Locker, Time saving in measurement of NMR and EPR relaxation times, Rev. Sci. Instrum. 41 (1970) 250–251.

[20] W.H. Hinson, W.T. Sobol, A new method of computing spin-lattice relaxation maps in magnetic resonance imaging using fast scanning protocols, Med. Phys. 15 (1988) 551–561.
[21] K. Scheffler, J. Hennig, T_1 quantification with inversion recovery TrueFISP, Magn. Reson. Med. 45 (2001) 720–723.
[22] K. Scheffler, Correction and calculation of T1 and T2 maps based on IR balanced SSFP using an analytical expression of the transient SSFP response, in: Proceedings of the International Society for Magnetic Resonance in Medicine, vol. 11, International Society for Magnetic Resonance in Medicine, 2003, p. 552.
[23] P. Schmitt, M.A. Griswold, P.M. Jakob, M. Kotas, M. Flentje, A. Haase, Quantification of both T1 and T2 with IR TrueFISP, in: Proceedings of the International Society for Magnetic Resonance in Medicine, vol. 11, International Society for Magnetic Resonance in Medicine, 2003, p. 135.